URBAN WATER JOURNAL, 2017
http://dx.doi.org/10.1080/1573062X.2016.1276811

Taylor & Francis
Taylor & Francis Group

RESEARCH ARTICLE

Development and performance of a parsimonious model to estimate temperature in sewer networks

Jorge A. Elías-Maxil[a], Jan Hofman[b,c], Bas Wols[b], Francois Clemens[a,d], Jan Peter van der Hoek[a,e] and Luuk Rietveld[a]

[a]Department of Water Management, Delft University of Technology, Delft, Netherlands; [b]KWR Watercycle Research Institute, Nieuwegein, Netherlands; [c]Water Innovation and Research Centre, University of Bath, Bath, UK; [d]Deltares, Delft, Netherlands; [e]Waternet, Amsterdam, Netherlands

ABSTRACT

This paper presents a model (inspired by another model) to calculate water temperature in free-surface flow with two main innovations: the convective heat transfer occurs only at the wetted perimeter of pipes, and the model was integrated to commercial software used for hydraulic calculations in drainage systems. Given these innovations, we could reduce the number of modeling input data to calculate the temperature of water and soil in the radial and tangential directions along the pipes, with the advantages of using industry-standard software. To test the performance of the model, it was firstly calibrated in two sets of experiments (to calibrate the hydraulic and the thermal parameters separately), and benchmarked with a third controlled discharge against the case model. The results indicate that in unsteady-state situations the parsimonious model can be twice as accurate as the underlying model because the parsimonious model considers the hydraulic influence of sewer infrastructure.

ARTICLE HISTORY
Received 4 October 2015
Accepted 11 July 2016

KEYWORDS
Heat recovery; wastewater temperature modeling; heat transfer

Introduction

Temperature plays an important role in processes that affect the infrastructure and operation of wastewater works. Based on data obtained from wet weather conditions and cold periods, Wanner *et al.* (2005) determined that a decrease of one degree Celsius in the liquid leads to a 10% reduction of the maximum specific net growth rate of nitrifying microorganisms. In sewer systems, high temperature accelerates processes involved in the sulfur cycle affecting the long term corrosion of pipes (Joseph *et al.* 2012) as well as the production of unpleasant odors and flammable gases (Yongsiri *et al.* 2004, Lahav *et al.* 2006). A study revealed that a change of 5 °C (from 20 to 25 °C) increased the sulfide oxidation by 15% (Nielsen *et al.* 2005).

Moreover, wastewater has been currently considered as a source of low-quality energy (sensible heat that can't be used to produce work) available in the surroundings of houses that can be used for ambient heating (Meggers and Leibundgut 2011); therefore, information about the availability and temperature distribution of water in sewer networks is needed.

Cipolla and Maglionico (2014) measured the flow and temperature of sewer networks at five sites for five months. The authors described the behavior of flow and temperature finding a relative variation from 0.25 to 1.5 times with respect to the mean daily flow, and 0.9 to 1.05 times with respect to the mean daily temperature of each monitoring site (from 20.9 °C in October to 13.5 °C in December).

Modeling tools have been developed to estimate the temperature change in gravity flow sewer pipes. Wanner *et al.* (2004) showed a model for water temperature along sewer conduits. Abdel-Aal *et al.* (2013) presented a simplified model to estimate the wastewater temperature in sewer pipes in steady-state conditions. Dürrenmatt and Wanner (2008) presented software called TEMPEST to estimate the temperature change in sewer pipes whose equations are also explained in a later paper (Dürrenmatt and Wanner 2014). In the TEMPEST model, the water temperature T_W [°C] is described by the balance shown in Equation (1) of the list of model equations in the supplementary material, the TEMPEST model takes into account the convective heat transfer from the pipe wall to the water in the wet part ($\dot{q}_{PW}\left[Js^{-1}m^{-2}\right]$) and the heat transfer from the surface water to air ($\dot{q}_{WL}$), the heat lost due to the change of phase of water by evaporation ($\dot{q}_{eW}$), as well as the heat gained by biologic metabolism inside the water per volume unit ($\dot{q}'_{COD}$). $\Omega_W[m]$, $cp_W[\mathrm{Jkg}^{-1}\mathrm{K}^{-1}]$, and $\rho_W[\mathrm{kgm}^{-3}]$ are the wetted perimeter, specific heat capacity and density of water respectively. V_W is the volumetric flow rate water and $B[m]$ stands for the width of the water surface.

Abdel-Aal *et al.* (2014) suggest that some of the parameters of the TEMPEST model are not sensitive, technically difficult to obtain and the software requires high computational load restricting its practical use and at the same time opening a gap in developing a parsimonious (reduced) model that can be used in a sewer network.

This paper presents a model that takes into consideration only the interactions governing heat transfer from water to the surroundings. The model was simplified with the results of the sensitivity analysis of the balance equations in the model TEMPEST,

CONTACT Jorge A. Elías-Maxil J.A.EliasMaxil@tudelft.nl
The supplemental material for this paper is available online at http://dx.doi.org/10.1080/1573062X.2016.1276811

presented by Dürrenmatt and Wanner (2014) and, simultaneously, another model was added to describe the temperature behavior of the soil surrounding a pipe. In order to calibrate it and test its performance in relation to the TEMPEST model, a series of controlled discharges was performed.

Methods

The research consisted of the development of the parsimonious model, and its calibration with the help of two separate experiments for the hydraulics and the thermal parameters needed. The parsimonious model was verified and compared to the TEMPEST model in steady and un-steady conditions with measurements obtained in a third set of experiments.

Model equations

In the developed parsimonious model (the equations are listed in the supplemental material), the St. Venant equations are also used to describe the flow in one dimension. The mass balance is read as in Equation (2), where $A_W[m^2]$ represents the cross sectional area of the wetted part of the sewer, $\dot{V}_W[m^3s^{-1}]$ is the volumetric flow rate of water. The variables $t[s]$ and $x[m]$ are the temporal and spatial coordinates of the system.

The momentum balance is described with Equation (3), where $h[m]$ is the water depth in the pipe g is the gravitational acceleration, C is the Chézy coefficient $[m^{1/2}s^{-1}]$ for friction resistance, $R_W[m]$ is the hydraulic radius given by the quotient A_W/Ω_W being Ω_W, $[m]$ the wetted perimeter and $S_O[m/m]$ is the sewer slope.

In turn, C is determined with a relation, based on the Strickler roughness coefficient k_s $\left[m^{1/3}s^{-1}\right]$. The relation is shown in Equation (4) of the supplemental material.

In the parsimonious model, the heat exchange is only governed by the heat conduction between the pipe and water along Ω_w of circular pipes as presented in Equation (5) of the list of equations. The balance neglects the heat transfer phenomena related to air in the headspace of the pipe. The reasons to exclude the heat transfer related to air are listed below.

In the TEMPEST model, it is assumed that air is incompressible and that there is free exchange of air between the in-sewer air and the atmosphere, which might not be accurate because some authors have concluded that the sewer ventilation is affected by the geometry of the systems (Granata *et al.* 2011); therefore, the convective heat transport by air was neglected.

The mass and heat exchange for the in-sewer air were also neglected since according to Dürrenmatt and Wanner (2014), the condensate that flows back to the water stream is small compared to the total water mass. Furthermore, the humidity in the headspace of sewer pipes near the case study was close to 100% according to our measurements and in agreement to typical values in sewers (Joseph *et al.* 2012), suggesting that evaporation-condensation processes are constantly in equilibrium.

Added to the exclusion of the air-related heat exchange, the metabolic heat production and the fouling factor were omitted since it has been shown the model is not sensitive to those parameters (Dürrenmatt and Wanner 2014); the most sensitive parameters were the soil temperature at the boundary condition ($T_{S,inf}$, [°C]), the thermal conductivity (λ_{S}, [Jkg^{-1}K^{-1}]) and the distance to the undisrupted soil (δ_S, [m]). Other sensitive parameters to model the water temperature in gravity flow are the input temperature and flow rate (Wanner *et al.* 2004).

Once the balance of the fluid is solved, $T_{W,out}$ is modeled with the heat balance (Equation (5)), which excludes the heat transfer from the surface water to air $\dot{q}_{WL}$, the heat lost due to evaporation of water $\dot{q}_{eW}$ and the generated heat due to microbial metabolism $\dot{q}'_{COD}$ is presented in Equation (1) in the TEMPEST model.

The heat flux at the interface water-pipe wall $\dot{q}_{PW}$ is given by the difference of temperature between the pipe wall (T_{Pw}), and the water (T_W), multiplied by a heat transfer coefficient $\alpha_{Pw}[Js^{-1}m^{-2}K^{-1}]$ according to Equation (6).

The heat transfer coefficient is given by Equation (7), where λ_W is the thermal conductivity of water ($\lambda_W = 0.6Js^{-1}m^{-1}K^{-1}$) and Nu is the dimensionless Nusselt number where $Nu = 0.023Re^{4/5}Pr^{1/3}$; Re and Pr are the dimensionless Reynolds and Prandtl numbers.

The heat conduction from the water to the pipe and from the pipe to the soil is modeled with an energy balance equation solved by the finite-differences method. The pipe and the soil are divided with a cross-sectional mesh (see Figure 1) into $i = 1, 2, \ldots$ to n layers in the radial direction (r), and $j = 1, 2, \ldots$to m tangential divisions of one vertical half of the pipe. The total number of layers in the radial direction (n) is given by the summation of n_p and n_s layers of the pipe and soil respectively. For a control element with volume $V[m^3]$ in the coordinates (i,j), the energy balance is given by the Equation (8).

From Equation (8), the rate of temperature change in the node (i, j) is given by the rate of temperature $\dot{E}[\text{kgm}^{-3}\text{s}^{-1}]$ transferred into V calculated as a rectangular prism by Equation (9), where $A'_{i,j}$ is the longitudinal area of the control volume with length $\Delta x[m]$ and radial distance from the pipe wall to the node $r_{i,j}[m]$. $A'_{i,j}$ is calculated with Equation (10).

$\dot{E}^r_{in}$ of Equation (8) indicates the incoming rate of temperature transferred in the radial direction. In the nodes that touch the wetted perimeter of the pipe, the heat transfer at the interface water-pipe wall is given by convection according to Equation (11) where $A'_{i,0}$ is also $\Omega_W * \Delta x$ at the nodes above the water level; $\dot{E}^r_{in,conv} = 0\text{kgm}^{-3}\text{s}^{-1}$.

After the first layer of the pipe to the boundary soil, the incoming radial heat conduction is given by Equation (12) where the term a is the thermal diffusivity [m^{2}s^{-1}] described by Equation (13) whose final value depends on the heat conductivity, the heat capacity and the density of the pipe and surrounding soil.

The tangential heat transfer is given by Equation (14). As the cross-sectional heat transfer is calculated for the vertical half of the pipe, it is assumed that there is adiabatic symmetry at the bottom (nodes i, 0) and the top (nodes i, m) of the half circumference.

Each increment of the radial distance is set according to Equation (15) where $K_{P|S}[-]$ is a factor of increment of the radial distance which varies for the pipe and the soil. Equation (15) implies that when $K > 1$, Δr_i increases proportionally to the distance from the center of the pipe. When $K = 1$, Δr is homogenous. In Equation (15), δ and n can become δ_p, n_p or δ_s, n_s for the pipe and soil respectively. The tangential length of each arc segment at the radial distance r_i is calculated with Equation (16). The initial temperature of both the pipe and the soil, $T_{P,0}$ and $T_{S,0}$, is also required.

At the wetted part of the pipe, the continuity conditions at the interface water-pipe (t, $r = D/2$, θ_W) are $T_W = T_{PW} = T^t_{i,0}$ implying that the heat transfer in the radial direction can be calculated from a partially-filled to full pipe flow with stagnant water. The

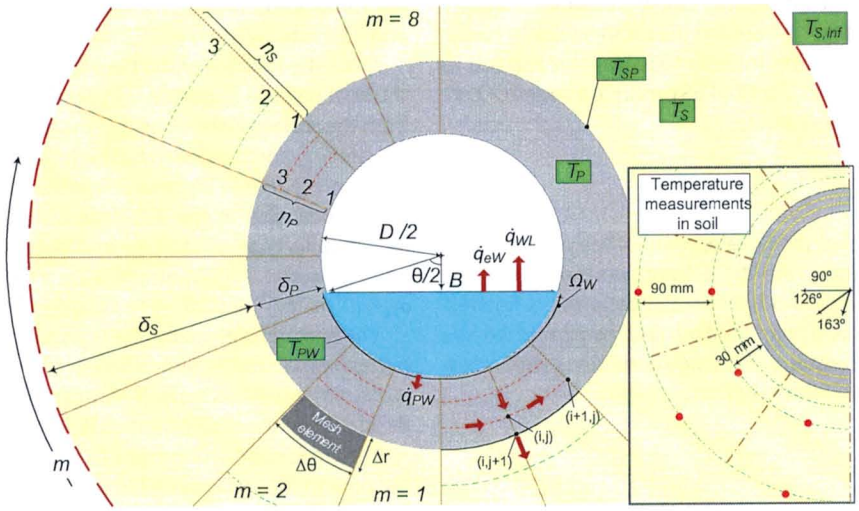

Figure 1. Cross section of pipe and surrounding soil; inspired by (Dürrenmatt and Wanner 2008)

continuity conditions at the interface pipe-soil $(t, r = D/2 + \delta_P, \theta_W)$ set the temperature of the pipe equal to the temperature of the interface $(T_P = T_{PS})$ and $\dot{q}_P = -\dot{q}_{PS}$ with the heat fluxes $\dot{q}_P$ and $\dot{q}_{PS}$ given by the Equations (17) and (18). At the end of the soil, the boundary conditions are $T_S(t, r = D/2 + \delta_P + \delta_S, \theta) = T_{S,inf}$.

In the tangential direction, the heat flux $\dot{q}_P$ at $(t, r, \theta = 0)$ is $-\dot{q}_P$ and $\dot{q}_S(t, r, \theta = 0) = -\dot{q}_S$. The temperature boundary conditions are: at $T_P(t, r, \theta = 0) = T_P$ and at $T_P(t, r, \theta = \pi r) = 0$.

In the longitudinal direction, the initial conditions of the heat transfer process at $(t = 0, x)$ are an initial water temperature $T_W = T_{W,0}$. At $(t, x = 0)$, the boundary condition for the upstream water temperature is $T_W = T_{W,in}$.

The parsimonious model has been developed as an add-on compatible with the urban drainage software Sobek™, allowing us to import sewer network databases, add manholes and other type of infrastructure, determine pump regimes, and modify any network in a graphical interface if required. It can be accessed at http://doi.org/10.4121/uuid:192e2343-8038-474d-893f-e0f4436c0c12.

The model can calculate temperature changes in water and soil in empty, partly filled of completely filled pipes varying the contact surface water in the pipe. Although a heat transfer model was not developed for other infrastructure elements different from conduits (manholes, pump stations, tanks) the storage capacity of other elements is considered in the hydraulic model.

Case study

The temperature model was tested in an empty sewer system located in the north of Amsterdam, constructed in 2007, with no connections. The average slope of the system (Figure 1a) is 0.62%. The pipes are made of PVC with an internal diameter D of 234 mm and 8 mm of thickness (δ_P), merging into the pipe from the manhole J to the pumping station, which has a diameter of 400 mm. All manholes have a diameter of 90 cm. At manhole J, there is a connection to another branch of the sewer. The pumping station at the downstream of the sewer has two identical pumps with a capacity of 10 Ls^{-1} each. Groundwater level measurements near the area indicated that the water table was between −2.9 and −2.65 m above sea level (masl). The profile view of the sewer is presented in Figure 1a of the supplemental material.

Hydrostatic readings of pressure and temperature of air and water (hydrostatic pressure readers DCX-22 from Keller™ with water level resolution of 25 *mmWC* and temperature accuracy of ± 0.5 °C) were taken every minute in the pipes near manholes B, C, D, E and H. The sensors were protected with a plastic hose with holes to avoid the effect of turbulence. A flow meter (Promag 50P, accuracy of 0.5% of measured flow) was installed at the discharge point, where periodical readings were done and the flow rate was controlled.

The soil temperature was measured at two places in the sewer pipe (S1 and S2 in Figure 1a) approximately at ¾ of the length between the pipe section A-B and the section D-E. The reason was to minimize the effect of turbulence caused by the discharge at the upstream manhole, and to guarantee the largest longitudinal heat exchange possible in the pipe without local disturbances caused by the manholes. The soil temperature was measured (with resistor temperature detectors; accuracy of ±0.21 °C) every minute in the cross sectional direction in the coordinates depicted in Figure 1 at two radial distances: 45 and 135 mm from the pipe wall.

In order to calibrate and validate the accuracy of the temperature model, the experimental work was divided into three main stages. The first stage embraced the calibration of the friction coefficient of the hydraulic model needed to determine the convectional heat transport in wastewater with a steady-state discharge. The second stage was the calibration of the conductive parameters that govern heat transfer from water to the surroundings. After the calibration of the heat transfer parameters, the model was validated and compared against TEMPEST.

Calibration of hydraulic and thermal parameters

Calibration of hydraulic parameters

For the hydraulic calibration, a constant flow of cold water was poured into the sewer from manhole A (Figure 1a). The

minimum value of the root mean squared error (RMSE) in Equation (19), (where Y and $\hat{Y}$ are the modeled and measured temperature respectively from $i = 1$ to N data pairs), at the conduits near the manholes B, C, D and H, was used as the target for the calibration. The calibration consisted of the adjustment for the hydraulic local losses of the manholes since it is expected that, according to preliminary calculations of flow velocity, the local losses are more important than hydraulic roughness to describe the flow rate at relatively low velocities (<2 ms^{-1}).

The local losses, interpreted as equivalent length ($L_{eq}[m]$), was the main calibration parameter of the hydraulic part of the model. The equivalent length was calculated for every manhole according to the relation shown in Equation (20) (Clemens 2001), where $\xi[-]$ represents a head loss coefficient calculated with Equation (21) (AASHTO 2005), $D_{mh}[m]$ represents the diameter of the manhole, Φ is the angle between the inflow and outflow pipes, $k_\Lambda[-]$ is a correction factor for free surface flow and $k_p[-]$ is a correction factor for plunging flow.

The factor k_Λ is given by Equation (22), while k_p is determined by Equation (23) where h_{mh}, [m] is the water depth in the manhole above the outlet of the pipe. The depths h and h_{mh} were calculated with a preliminary model using a k_S value of 63 $m^{1/3}s^{-1}$. The applied optimization method to adjust L_{eq} in each manhole of the model was the Nelder-Mead method.

Calibration and uncertainty of thermal parameters

For this calibration, the sewer was blocked at manhole E (Figure 1a), and filled up in less than 30 min from manhole A with hot water. The temperature at the manholes B, C and D, plus the soil temperature at points S1 and S2 in Figure 1a was measured every minute for more than six hours to observe the cooling rate of the water in the pipe and soil and, in that way, to calculate the thermal properties of the system. The hot water was provided by the cooling towers of an industrial site, and transported to the location of the experiment. In order to install the sensors in the soil, the soil was dug at points S1 and S2 more than three weeks before the experiments started, to let the soil properties be restored and thus avoid systematic measurement errors due to soil disruptions. It was assumed that there is low uncertainty between geometry of the database in the model and the actual dimensions of the sewer system.

Since the parsimonious model for temperature is influenced by eleven variables, the calibration procedure firstly consisted of a parameterization process to reduce the parameters to be calibrated followed by a Monte Carlo method, based on a Bayesian Network. The optimization parameter was to find the minimum RMSE of water at three positions along the sewer required to calibrate the model, and to determine the uncertainty of the calibrated parameters.

For the parameterization, it was assumed that the thermal properties of the PVC pipes do not change significantly from the literature values, therefore; $cp_p = 1005\,Jkg^{-1}K^{-1}$, $\lambda_p = 0.14\,Js^{-1}m^{-1}K^{-1}$, $\rho_p = 1375\,kgm^{-3}$, based on Bishop (1978) and Abu-Hamdeh (2003). The thermodynamic characteristics of water were set as $cp_W = 4183\,Jkg^{-1}K^{-1}$ and $\rho_W = 1000\,kg\,m^{-3}$. $T_{s,inf}$ was set to the average measured value at points S1 and S2 (12.4 °C).

Another parameter that was fixed before calibration was the thickness of the modeled soil layer (δ_S) because the position of the installed sensors in the soil was fixed too. The distance of the sensors (Figure 1) was determined based on a preliminary heat balance performed in a simulated PVC pipe of 100 m length and 234 mm diameter with similar soil characteristics. In the balance: $T_S \approx T_{S,inf}$ when $\delta_S \approx 2$ m thus, δ_S was set to 2.61 m to keep an optimum balance between the distance to the undisrupted soil and the distance between the position of the sensors and the point of the mesh where the soil temperature is modeled. The increment factors were $K_p = 1$ and $K_S = 3$.

The remaining parameters ρ_S, cp_S and λ_S (density, specific heat and thermal conductivity of the soil) were therefore the calibrated parameters. Additionally, these three parameters are related with Equation (13), to determine the thermal diffusivity of the soil (a_S). This implies that the calibration can depend of a single variable, and there is more than one combination of ρ_S, cp_S and λ_S that can lead to the calibrated value of a_S.

In order to find the calibrated values of ρ_S, cp_S, and λ_S, the three parameters were varied according to random, uniformly distributed values generated inside the ranges 1440–2080 kgm^{-3}, 830–1550 $Jkg^{-1}K^{-1}$ and 1–3 $Js^{-1}m^{-1}K^{-1}$ respectively; taking into account thermal properties in moist and compacted soils (Ekwue *et al.* 2006, Smits *et al.* 2009, Tarnawski *et al.* 2011). The frequency distribution and confidence interval of a_S were estimated with a Bayesian Network according to Equation (13).

Validation and comparison with TEMPEST

The validation and comparison with TEMPEST (version 1.02) consisted in the analysis of residuals of water temperature at manholes B, E and H of controlled discharges of hot water poured into the sewer from manhole A, to the pump station in partially-filled flow. Between every controlled discharge there was a resting time of approximately two hours to cool down and drain the pipes as much as possible. The flow rate at each discharge was kept at 6 Ls^{-1} for approximately 30 min (36 m^3 of water in total) and 50 °C. The flow rate and temperature were chosen such that the sensors in the sewer pipe were always in contact with water, and to obtain the highest temperature difference between the soil and water possible.

For the comparison of the parsimonious model against TEMPEST, we took account of three considerations concerning the values of input data that both models will use: Since the number of input data for TEMPEST is larger than our model, the first consideration was to use measured input data in TEMPEST whenever possible therefore; the input data ambient temperature ($T_{amb} = 11.2°C$), ambient relative humidity ($\varphi = 1$) and ambient air pressure ($p_{amb} = 1013\,mbar$] were obtained from measurements *in situ* and from meteorological data. The second consideration was to assume a value to those parameters difficult to measure therefore, air exchange coefficient (b, [−]), COD degradation rate (r_{COD}, [$0.0001 mgCOD \cdot m^3 s^{-1}$] were set to 1.0 and 0.001 respectively. The implications of changing these parameters was assessed in a published sensitivity analysis (Dürrenmatt and Wanner 2014) and own calculations. The results let us know that the variation of φ, b, r_{COD} and p_{amb} to more than the double or to the opposite value, changes less than 1% from the output water temperature in TEMPEST.

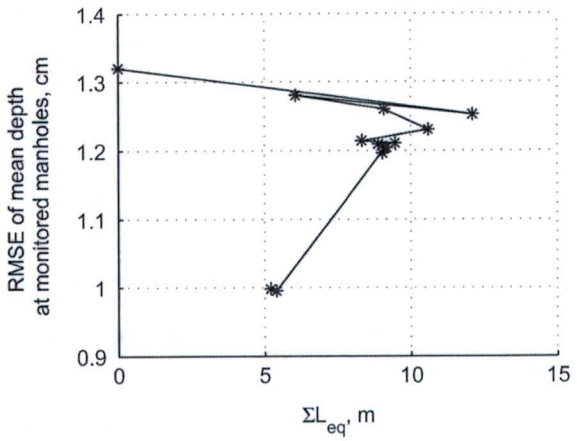

Figure 2. Optimization path of the hydraulic calibration of the reduced model.

Results

Calibration

Hydraulic calibration

In agreement with the Equations (20) to (23) and the head loss measurements, the equivalent length (L_{eq}) in each manhole was calculated. The summation of L_{eq} for the entire sewer system was approximately 12 m, with manhole E being the place in the sewer with the largest local loss (7 m) because the mentioned manhole is a corner with an angle Θ of 90 degrees. Manholes B and D were the second and third structures that contributed to the local losses (4 m and 1 m respectively). Since the remaining manholes contributed for less than 1 m, they were discarded from the adjustments. In order to reach an optimum ΣL_{eq}, a total of 13 simulations were performed to reach a minimum RMSE of the average depth at the monitored manholes (Figure 2). The optimum ΣL_{eq} was approximately 5.4 m. The water level measurements in manhole D showed more noise than the other manholes. This situation may be a result of the turbulence caused by the height difference between the inlet and the outlet in the manhole (70 cm). This measurement was excluded from the data used for the hydraulic calibration.

Calibration and uncertainty of thermal parameters

According to the Bayesian analysis, the optimal a_s was 0.862 × 10^{-6} m^2s^{-1} (upper right histogram of Figure 3) from the combination of $\lambda_s = 1.9\,Js^{-1}m^{-1}K^{-1}$, $cp_s = 1276\,Jkg^{-1}K^{-1}$ and $\rho_s = 1733\,kgm^{-3}$ in Equation (13) therefore, these previously mentioned values of λ_s, cp_s and ρ_s were taken as calibrated values for the parsimonious model and the calibrated value of a_s was the corresponding calibrated input in TEMPEST.

The mean value of a_s according to the Bayesian analysis was approximately 1.02 × 10^{-6} m^2s^{-1} which is different to the calibrated value of 0.862 × 10^{-6} m^2s^{-1}. The reason is that in the procedure to propagate λ_s, cp_s and ρ_s the probability to choose any number within their respective ranges was uniform. However, the calibrated value appeared near the mean value of the confidence interval modeled with the Bayesian analysis. According to the calibrated value of a_s, the calibrated values of λ_s, cp_s and ρ_s were 1.9 J · s^{-1} m^{-1} K^{-1}, 1276 J · kg^{-1} K^{-1}, and 1733 kgm^{-3} respectively.

The measured and modeled water temperature with the calibrated values is depicted in Figure 4. The average RMSE of the calibrated water temperature at the monitored sites was 1.45 °C. The largest error was observed in the pipe close to manhole D (RMSE = 1.88 °C) mainly because at the beginning of the experiment the water heated faster than the modeled results. The RMSE in manholes B and C was approximately 1.22 °C and 1.27 °C respectively. The average RMSE can be considered high,

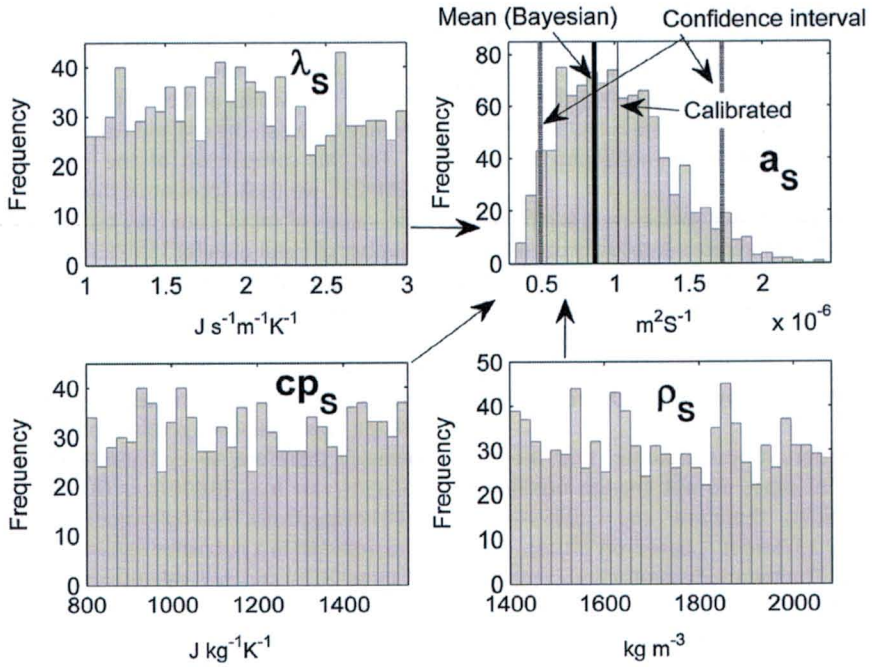

Figure 3. Bayesian analysis to calibrate a_s from the frequency distributions of λ_S, cp_S and ρ_S.

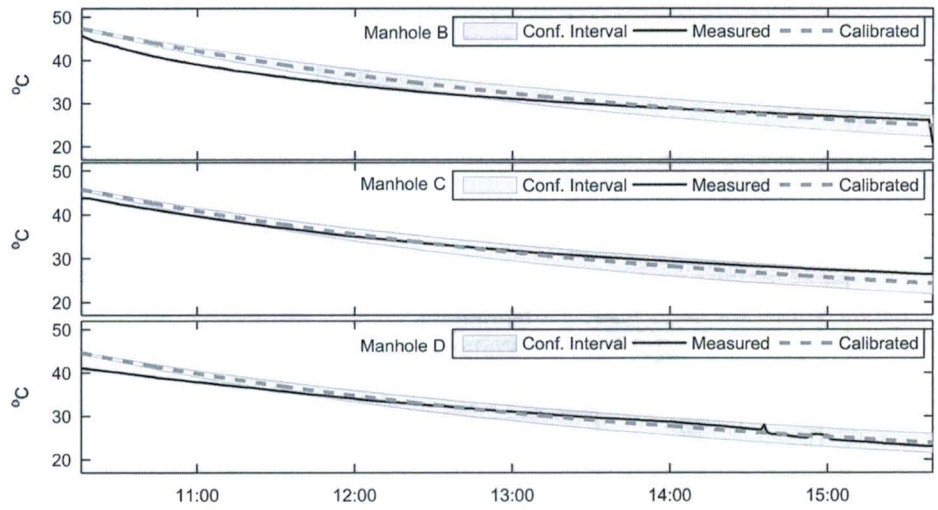

Figure 4. Simulated and observed water temperature near manholes B, C and D during the calibration of the thermal properties of the soil; uncertainty of water temperature by the Bayesian Analysis at 95% of confidence level.

particularly when the temperature difference between comparison points (Manhole B, C and D) is a few degrees Celsius. However, according to the uncertainty of a_s from the Bayesian analysis, the measured water temperature fitted inside the interval at 95% confidence level (Figure 4) excepting the first two hours of the experiments after the pipe was filled with water, in that time, the registered water temperature was lower than expected by the model. A reason for that could be the unaccounted heat transferred to the air (evaporation, heat lost in the water surface, and heat loss in the non-wetted perimeter) replaced by water at the beginning of the experiment.

Figure 5 depicts the box plots during the standardized residuals at all measurement points in water and soil. The standardized residuals are defined as the coefficient between the residuals ($\in_i = Y_i - \hat{Y}_i$) and their standard deviation. In each box, the line that divides them represents the median value, the end of the box on each side is the value of the first quartile and the end of the lines shows the limit value of the second quartile of the residuals. The dots beyond the box represent the outliers. In the middle sub-plot of Figure 5, the standardized residuals of water temperature at the manholes B, C and D are shown. It can be seen that the median of the residues in manhole B and D is close to the 0 value, suggesting that there is a balance between the negative and positive residues obtained. The symmetry of the box plots of the three manholes indicate that the residuals were distributed evenly in a positive and negative direction in the first quartile of the residuals.

The modeled soil temperature diverged at both measurement points (upstream at S1, and downstream at S2). At the upstream (S1), the medians of the nearest layer to the pipe (1_1, 1_2 and 1_3) were closer to the zero value than the second layer (2_1, 2_2, 2_3). Both layers were skewed to the negative side, meaning that the modeled soil temperature was higher than the measured temperature. The symmetry of the boxes as well as the distance of the quartiles to the median are similar between layers, which implies that there can be a systematic deviation caused by a missing description in the model or a parameter's values. The residuals in the downstream measurement point S2 (lower subplot of Figure 5), do not show a large systematic deviation as in S1. In the first layer of S2, all medians were positive and most parts of the boxes and the lines of the first quartile are also on the positive side, suggesting that the modeled temperature was lower than the measured temperature.

The first source of inaccuracy was to consider the characteristics of the soil as isotropic, in that sense, the average soil temperature between S1 and S2, differed by almost two degrees Celsius. The standard deviation of the initial temperature in the radial direction (see Figure 1) at the points S1 and S2 was similar (0.3 °C and 0.4 °C respectively) suggesting that the quality of the measurements was similar at both sites. One cause of the temperature difference can be explained by the ground water level; during an inspection of the sewer, we noticed groundwater infiltration at the bottom of manhole D (repaired before the experiments took place) at 0.2 masl, which is approximately five centimeters higher than the level of the location S2 at the time that the sensors were placed, the soil was only moist. The distance between manhole D and S2 is around 34 m (Figure 1a). Moreover, the groundwater level can also modify the thermal characteristics of the soil. Sallanko and Pekkala (2008) considered that groundwater significantly enhances the thermal conductivity of soil, and hence could potentially increase ground source heat exchange by several times for a fixed temperature gradient. As it is not possible to consider the soil as anisotropic in the parsimonious model, the mean value of all the soil readings at time 0 was set to one single average value $T_{s,0}$. Additionally, it is possible that the distance between the calculation nodes of the mesh was large, decreasing the accuracy of the model for the soil temperature. Although a smaller mesh can increase the accuracy, we decided to keep few segments in the mesh due to the computational load needed to model large sewer pipes, and because the main objective of the model is to estimate the water temperature. Moreover, in order to model the soil temperature around the pipes accurately, there are other processes to consider such as the resolution of the equipment (it is expected that with the current sewer temperature, there is not a large temperature variation in the soil around the pipes compared to the soil a few meters away) and noise (such as solar radiation and ambient temperature, groundwater).

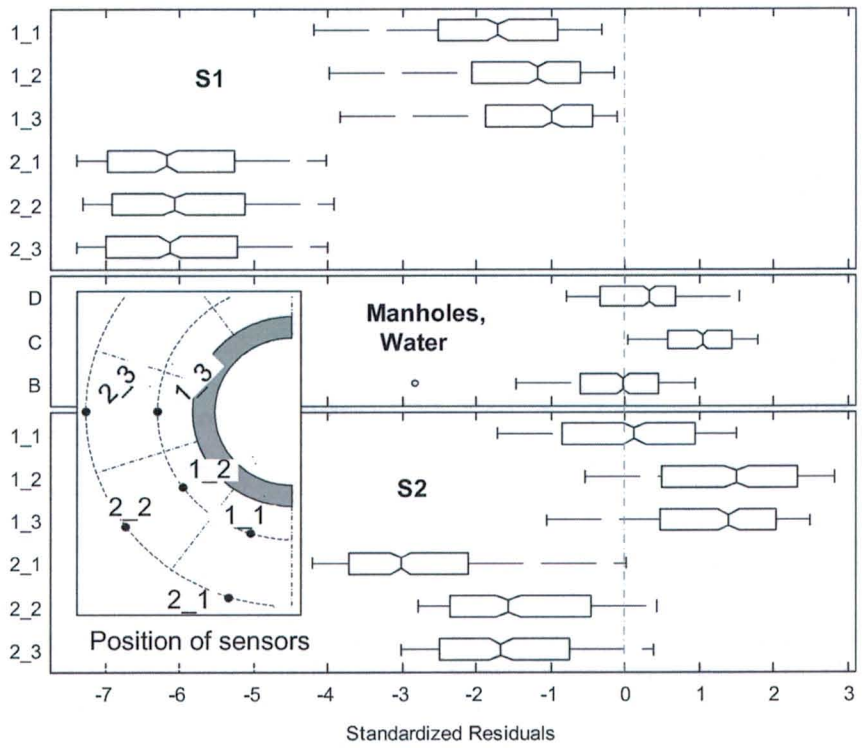

Figure 5. Standardized residuals of water and soil temperatures during the calibration of thermal parameters of the parsimonious model.

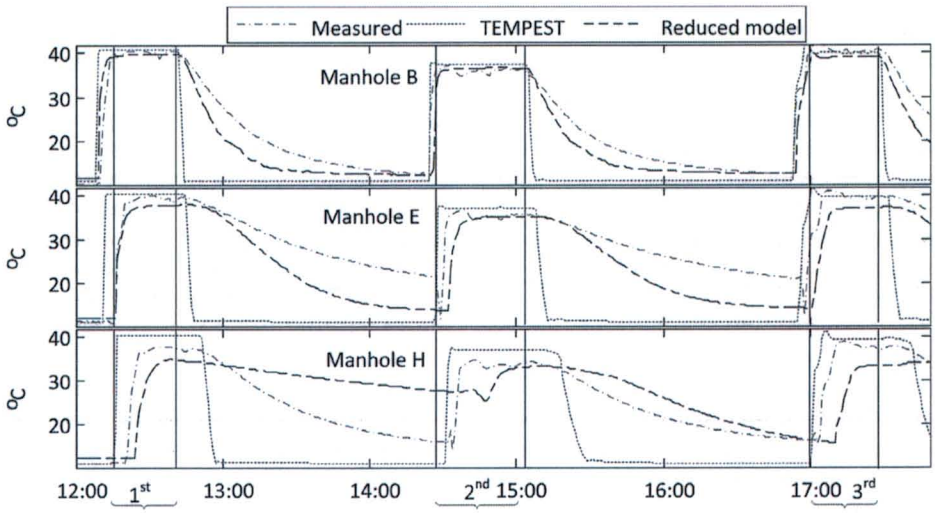

Figure 6. Observed and simulated water temperature at different manholes. Braces represent the time of water discharge.

Validation and comparison

When the model TEMPEST and the parsimonious model were compared in steady-state conditions, both presented similar accuracy with TEMPEST being slightly more accurate than the parsimonious model (RMSE of TEMPEST = 1.8 °C while RMSE of parsimonious model = 2.0 °C), especially at manhole H (RMSE of TEMPEST = 2.9 °C while RMSE of parsimonious model = 3.2 °C) where the modeled temperature by the parsimonious model had a time mismatch. An explanation is that the storage at the end of the sewer by the connection at manhole H could have modified the modeled water depth and hence the heat exchange. Another reason is that TEMPEST considers the heat exchange related to the air.

For un-steady conditions the RMSE of TEMPEST increased to 11.5 °C while for the parsimonious model, the RMSE augmented more than the double (5.3 °C) because the parsimonious model described more accurately the flow in-between discharges than TEMPEST due to the consideration of the hydraulic influence of manholes, other empty space and the pump regime. The RMSE of

the steady-state comparison and the graphic results can be seen in Figure 6 which illustrates the measured and modeled water temperature with TEMPEST and the current reduced model, at the outlet of manholes B, E and H. It was observed that from manhole B to H (237 m of distance between both), the water temperature decreased approximately four degrees Celsius. The computation time to solve the parsimonious model was approximately six times less than the time needed to solve the same model in TEMPEST on the same computer.

The performance at manhole E of both models, was the lowest compared to the remaining manholes, possibly due to a drawback of 1D models to describe the hydraulics to describe some conditions in certain structures (Leandro *et al.* 2009).

The largest source of inaccuracy during the experiment was found in the synchronization time of the filling and emptying stages of the discharges. Similar findings have been shown by Clemens (2001) when, during the calibration of a hydraulic model in a drainage area, the bias was higher during the emptying stage.

The analysis of residuals of both models for water temperature and soil temperature (for the parsimonious model) is shown in Table 1a of the supplemental material together with the empirical and theoretical cumulative probability distribution functions (CFD) of the water temperature residuals of TEMPEST and the parsimonious model, for the manholes B, E and H (Figure 2a of the supplemental material). For water temperature, the mean squared error (MSE) and the mean variance of the parsimonious model are lower than in TEMPEST. The bias of the parsimonious model, calculated as the square of MSE minus the mean of the variance, as in Equation (24) is approximately one half of the bias in TEMPEST. Because of the ranges in soil temperature, the value of MSE and the variance; the bias of soil temperature of the parsimonious model can be considered high, a method to decrease those numbers are the consideration of a heterogeneous soil and the decrease of the mesh in the soil.

Conclusions

In order to reduce the amount of input data needed to model the water temperature in free-surface flow, a model that neglects the air-related processes of heat exchange in pipes was developed. In order to know the wetted perimeter and velocity of a modeled discharge in pipes (needed in the temperature model), the parsimonious model was integrated to industry-standard software.

The use of controlled discharges to calibrate the hydraulic and thermal parameters of the model separately offered us the advantage of distinguishing some sources of inaccuracy. The equivalent length of pipes connected in a manhole at different levels was difficult to measure due to turbulence. The sensitivity of the hydraulic parameters to the final temperature in the water and the soil is unknown.

The full pipe method to calibrate the thermal characteristics of the soil can be used when the model is going to be applied on another site; an advantage of this method is that experimental costs and environmental burdens are diminished since no continuously flowing water is needed. A method to determine the soil boundary thickness can improve the calibration of the model.

The anisotropic characteristics of the soil (in the initial temperature conditions and thermal characteristics) as well as the soil discretization, decreased the accuracy of the model to calculate the water and soil temperature.

For water temperature, the comparison of the developed temperature model against TEMPEST showed similar results for steady state condition and an improvement of approximately double in transient conditions, where the largest errors were caused by the inaccuracy in the filling and emptying stages of the discharges. The inaccuracy of the parsimonious model was reduced thanks to the fact that the commercial software where the model is integrated, calculates the changes of flow behavior caused by sewer infrastructure (manholes, empty pipes and pumping stations).

Nomenclature and list of model equations

Nomenclature

A_W	Cross sectional area of pipe (Water), $[m^2]$
a	Thermal diffusivity, $[m^2 s^{-1}]$
A'	Lateral area to the pipe, $[m^2]$
b	Air exchange coefficient, [-]
B	Width of water surface, $[m]$
C	Chezy coefficient, $[m^{1/2}s^{-1}]$
cp_W, cp_P, cp_S	Heat capacity (Water, Pipe, Soil), $[Jkg^{-1}K^{-1}]$
D, D_mh	Diameter (Nominal, manhole), $[m]$
$\dot{E}^r, \dot{E}^\theta$	Radial and tangential temperature transfer, $[m^3 K s^{-1}]$
g	Gravitational force, $[9.81\ m^2 s^{-1}]$
h, h_{mh}	Water depth (Pipe, at manhole above the outlet pipe), $[m]$
i, j	Index in radial and tangential coordinates
K_P, K_S	Thickness factor (Pipe, Soil), [-]
k_A, k_P	Correction factor (free surface, plunging flow), [-]
k_s	Strickler friction coefficient, $[m^{1/3}s^{-1}]$
L_{eq}	Equivalent length, $[m]$
m	Total number of tangential sectors, [-]
n_P, n_S	Total number of radial layers (Pipe, Soil), [-]
N	Total number of observations
Nu	Nusselt number, [-]
p_{amb}	Ambient pressure, $[mbar]$
Pr	Prandtl number, [-]
$\dot{q}_{PW}, \dot{q}_{WL}, \dot{q}_{eW}\, \dot{q}_P, \dot{q}_{PS}, \dot{q}_S$	Heat flux/area (Water-pipe wall, water-air, evaporation, pipe, pipe-soil, soil), $[Js^{-1}m^{-2}]$
$\dot{q}'_{COD}$	Heat flux/ volume (Metabolism), $[Js^{-1}m^{-3}]$
r	Radial distance/coordinate from the center of the pipe, $[m]$
r_{COD}	COD degradation rate, $[mg_{COD}m^{-3}s^{-1}]$
Re	Reynolds number, [-]
R_W	Hydraulic radius, $[m]$
So	Sewer slope, $[m/m]$
$T_W, T_{PW}, T_P, T_S\, T_{S,\text{inf}}, T_{amb}, T_L$	Temperature (Water, Pipe wall, Pipe, Soil, Boundary, Ambient, In-sewer air), [°C]

t	Time, $[s]$
V	Volume, $[m^3]$
$\dot{V}_W$	Volumetric flow rate (Water), $[m^3 s^{-1}]$
x	Spatial coordinate in the longitudinal direction, $[m]$
Y	Given measured variable
$\hat{Y}$	Given modeled (estimated) variable
α_{PW}	Heat transfer coefficient (Pipe wall), $[Js^{-1}m^{-2}K^{-1}]$
δ_P, δ_S	Thickness (Pipe, Soil), $[m]$
$\in$	Residual of given variable, [-]
$\mathbf{\Phi}$	Angle between inflow and outflow pipes, $[rad]$
θ_W	Wetted tangential segment, [-]
$\lambda_W, \lambda_P, \lambda_S$	Thermal conductivity (Water, Pipe, Soil), $[Js^{-1}m^{-1}K^{-1}]$
ξ	Head loss coefficient, [-]
ρ_W, ρ_P, ρ_S	Density (Water, Pipe, Soil), $[kgm^{-3}]$
φ	Ambient relative humidity, [-]
$\mathbf{\Omega}_W$	Perimeter (Wetted), $[m]$

List of equations

Water temperature balance in TEMPEST model.

$$\frac{\partial(A_W T_W)}{\partial t} = \frac{\partial(\dot{V}_W T_W)}{\partial x} + \frac{1}{cp_W \rho_W}(\dot{q}_{PW}\Omega_W - \dot{q}_{WL}B - \dot{q}_{eW}B + \dot{q}'_{COD}A_W) \tag{1}$$

One dimensional mass balance of St. Venant equations.

$$\frac{\partial A_W}{\partial t} + \frac{\partial \dot{V}_W}{\partial x} = 0 \tag{2}$$

One dimensional momentum balance of St. Venant equations.

$$\frac{\partial \dot{V}_W}{\partial t} + \frac{\partial}{\partial x}\left(\frac{\dot{V}_W^2}{A_W}\right) + gA_W\frac{\partial h}{\partial x} + \frac{g|\dot{V}_W|\dot{V}_W}{C^2 R_W A_W} - gA_W S_O = 0 \tag{3}$$

Hydraulic friction resistance used in Equation (3).

$$C = k_s R_W^{1/6} \tag{4}$$

Parsimonious temperature balance equation inspired by Equation (1).

$$\frac{\partial(A_W T_W)}{\partial t} + \frac{\partial(\dot{V}_W T_W)}{\partial x} - \frac{\dot{q}_{PW}\Omega_W}{cp_W \rho_W} = 0 \tag{5}$$

Heat flux at the interface water-pipe wall.

$$\dot{q}_{Pw} = \alpha_{Pw}(T_W - T_{Pw}) \tag{6}$$

Heat transfer coefficient of Equation (6).

$$\alpha_{Pw} = \frac{Nu \cdot \lambda_W}{R_W} \tag{7}$$

Parsimonious temperature balance equation for conduction of heat in the radial and tangential direction of the pipe and surrounding soil.

$$V_{i,j}\frac{T_{i,j}^{t+\Delta t} - T_{i,j}^{t}}{\Delta t} = \dot{E}_{in}^{r} + \dot{E}_{in}^{\theta} + \dot{E}_{out}^{r} + \dot{E}_{out}^{\theta} \tag{8}$$

Volume of a control element (mesh element in Figure 1).

$$V_{i,j} = \Delta r_{i,j} \cdot A'_{i,j} \tag{9}$$

Longitudinal area of a control element.

$$A'_{i,j} = \frac{\Delta x \cdot \pi \cdot r_{i,j}}{m} \tag{10}$$

Radial heat transfer at interface water-pipe wall (at $n_P = 1$ of the wetted perimeter)

$$\dot{E}_{in,conv}^{r} = A'_{i,0} \cdot \frac{\alpha_{Pw}}{\rho_P cp_P}(T_W^t - T_{i,0}^t) \tag{11}$$

Radial heat transfer at interface water-pipe wall (at $n_P > 1$ and any n_S).

$$\dot{E}_{in,cond}^{r} = \frac{A_{i,j} \cdot a}{\Delta r_{i,j}}(T_{i,j-1}^t - T_{i,j}^t) \tag{12}$$

Heat diffusivity of pipe and soil.

$$a = \frac{\lambda}{cp \cdot \rho} \tag{13}$$

Tangential heat transfer by conduction in the pipe and soil.

$$\dot{E}_{in,cond}^{\theta} = \frac{A_{i,j} \cdot a}{\Delta\theta_{i,j}}(T_{i,j}^t - T_{i-1,j}^t) \tag{14}$$

Radial distance of a control volume (mesh element in Figure 1).

$$\Delta r_{i,j} = \frac{\delta}{\sum_{i=1}^{n} K_{P|S}^{i-1}} \cdot K_{P|S}^{i-1} \tag{15}$$

Tangential distance of a control volume (mesh element in Figure 1).

$$\Delta\theta_{i,j} = \frac{\pi}{m}\frac{(r_i + r_{i+1})}{2} \tag{16}$$

Heat flux at the interface water-pipe for continuity conditions.

$$\dot{q}_P = -\left(\lambda_p \frac{\partial T_{PW}}{\partial r}\right) \tag{17}$$

Heat flux at the interface pipe-soil for continuity conditions.

$$\dot{q}_{PS} = -\left(\lambda_S \frac{\partial T_S}{\partial r}\right) \tag{18}$$

Equations (19) to (24): equations used in the calibration and verification of the parsimonious model.

$$RMSE = \sqrt{\frac{1}{N-1}\sum_{i=1}^{N}(Y_i - \hat{Y}_i)^2} \tag{19}$$

$$L_{eq} = \frac{\xi \cdot C^2 \cdot R_W}{2g} \tag{20}$$

$$\xi = \left[0.1\left(\frac{D_{mh}}{D}\right)(1 - \sin\Phi) + 1.4\left(\frac{D_{mh}}{D}\right)^{0.15} \cdot \sin\Phi\right] \cdot k_\Lambda \cdot k_P \tag{21}$$

$$k_{\Lambda} = 0.5 \cdot \left(\frac{h}{D}\right)^{0.6} \quad (22)$$

$$k_{p} = 1 + 0.2 \cdot \left(\frac{h}{D}\right)\left(\frac{h - h_{mh}}{D}\right) \quad (23)$$

$$Bias = \sqrt{\frac{1}{N}\sum_{i=1}^{N} \epsilon_i^2 - \left(\epsilon_i - \dot{\epsilon}\right)^2} \quad (24)$$

Acknowledgements

The authors thanks to Waternet for the facilities provided for the experiment as well as CONACYT for the scholarship received by J. E. M. during this research.

Disclosure statement

No potential conflict of interest was reported by the authors.

Funding

This work was supported by Consejo Nacional de Ciencia y Tecnologia [grant number 205249].

References

AASHTO, 2005. *Model drainage manual*. 3rd ed. Washington, DC: American Association of State and Highway Transportation Officials.

Abdel-Aal, M., et al., 2013. Viability of heat recovery from combined sewers. *In: 7th International Conference on Sewer Processes & Networks*, August 2013. Sheffield: IWA, 28–30.

Abdel-Aal, M., et al., 2014. Modelling the viability of heat recovery from combined sewers. *Water Science & Technology*, 70 (2), 297–306.

Abu-Hamdeh, N.H., 2003. Thermal properties of soils as affected by density and water content. *Biosystems Engineering*, 86 (1), 97–102.

Bishop, R.R., 1978. *Hydraulic characteristics of PVC pipe in sanitary sewers (A report of field measurements)*. Logan, UT: Utah Water Research Laboratory.

Cipolla, S.S. and Maglionico, M., 2014. Heat recovery from urban wastewater: Analysis of the variability of flow rate and temperature. *Energy and Buildings*, 69, 122–130.

Clemens, F.H.L.R., 2001. *Hydrodynamic models in urban drainage: Application and calibration*. Delft: Delft University of Technology.

Dürrenmatt, D.J. and Wanner, O., 2008. Simulation of the wastewater temperature in sewers with TEMPEST. *Water Science and Technology*, 57, 1809–1815.

Dürrenmatt, D.J. and Wanner, O., 2014. A mathematical model to predict the effect of heat recovery on the wastewater temperature in sewers. *Water Research*, 48 (1), 548–558.

Ekwue, E.I., Stone, R.J. and Bhagwat, D., 2006. Thermal conductivity of some compacted trinidadian soils as affected by peat content. *Biosystems Engineering*, 94 (3), 461–469.

Granata, F., et al., 2011. Hydraulics of circular drop manholes. *Journal of Irrigation and Drainage Engineering*, 137 (2), 102–111.

Joseph, A.P., et al., 2012. Surface neutralization and H2S oxidation at early stages of sewer corrosion: Influence of temperature, relative humidity and H2S concentration. *Water Research*, 46 (13), 4235–4245.

Lahav, O., Sagiv, A. and Friedler, E., 2006. A different approach for predicting H2S(g) emission rates in gravity sewers. *Water Research*, 40 (2), 259–266.

Leandro, J., et al., 2009. Comparison of 1D/1D and 1D/2D coupled (sewer/surface) hydraulic models for urban flood simulation. *Journal of Hydraulic Engineering*, 135 (6), 495–504.

Meggers, F. and Leibundgut, H., 2011. The potential of wastewater heat and exergy: Decentralized high-temperature recovery with a heat pump. *Energy and Buildings*, 43 (4), 879–886.

Nielsen, A.H., Hvitved-Jacobsen, T. and Vollertsen, J., 2005. Kinetics and stoichiometry of sulfide oxidation by sewer biofilms. *Water Research*, 39 (17), 4119–4125.

Sallanko, J. and Pekkala, M., 2008. Wastewater temperature decrease in pressure sewers. *Water Environment Research*, 80 (12), 2247–2252.

Smits, K.M., et al., 2009. Determination of the thermal conductivity of sands under varying moisture, drainage/wetting, and porosity conditions-Applications in near-surface soil moisture distribution analysis. *In: Proceedings from Hydrology Days*, March 2009. Fort Collins, CO: Colorado State University, 57–65.

Tarnawski, V.R., Momose, T. and Leong, W.H., 2011. Thermal conductivity of standard sands II. Saturated conditions. *International Journal of Thermophysics*, 32 (5), 984–1005.

Wanner, O., Panagiotidis, V. and Siegrist, H., 2004. Wärmeentnahme aus der kanalisation-einfluss auf die abwassertemperatur [Heat recovery from sewers: Effect on the wastewater temperature]. *Korrespondenz Abwasser*, 51 (5), 489–495.

Wanner, O., et al., 2005. Effect of heat recovery from raw wastewater on nitrification and nitrogen removal in activated sludge plants. *Water Research*, 39 (19), 4725–4734.

Yongsiri, C., Vollertsen, J. and Hvitved-Jacobsen, T., 2004. Effect of temperature on air-water transfer of hydrogen sulfide. *Journal of Environmental Engineering*, 130 (1), 104–109.